

Acoustic modes and elastic properties of polymeric nanostructures

R. D. Hartschuh, A. Kisliuk, V. Novikov,^{a)} and A. P. Sokolov^{b)}
Department of Polymer Science, University of Akron, Akron, Ohio 44325

P. R. Heyliger
Department of Civil Engineering, Colorado State University, Fort Collins, Colorado 80523

C. M. Flannery and W. L. Johnson
Materials Reliability Division, NIST, Boulder, Colorado 80305-3328

C. L. Soles and W.-L. Wu
Polymers Division, NIST, Gaithersburg, Maryland 20899-8541

(Received 1 April 2005; accepted 1 September 2005; published online 21 October 2005)

Phonon spectra of polymeric linear nanostructures have been characterized using Brillouin light scattering. In addition to phonon modes similar to those present in uniform thin films, the phonon spectra of the nanolines reveal a new mode with a lower frequency that depends on the width of the nanolines. Classic wave theory and finite element analysis were combined to identify this new mode as a flexural vibration of the nanolines. Analysis of the phonon spectra gave estimates of elastic constants in the nanostructures and indicated that there is no significant deviation from bulk mechanical properties and no mechanical anisotropy in structures as small as 88 nm. © 2005 American Institute of Physics. [DOI: 10.1063/1.2119414]

Mechanical properties and the stability of nanostructured materials are of paramount importance for a wide range of emerging applications that span microelectronic, photonic, nano-electro-mechanical systems, nanofluidic, and biomedical technologies. At the nanoscale, forces that are negligible in macroscopic systems, such as surface tension, often become significant. An example that is critically important to semiconductor fabrication is the ability of a nanostructure to resist buckling or collapse, since the capillary forces from a rinsing liquid can destroy patterns.¹⁻⁴ Polymers are often used to fabricate nanostructures, either directly or indirectly through a resist process. However, polymers are susceptible to material property deviations when the relatively large macromolecules, random coils on the order of (5–50) nm, are confined to structures that approach these dimensions.⁵⁻⁸ In particular, recent simulations suggest that Young's modulus of lithographically patterned polymer nanostructures decreases and becomes anisotropic when the feature size becomes comparable to a few (approximately 3) molecular diameters.⁴ Such a modulus reduction would magnify the instability of structures fabricated at these length scales. Therefore, direct measurements of elastic properties in polymeric nanolines are important for successfully modeling and optimizing the mechanical behavior. Currently there is no reliable experimental method that can provide information on mechanical properties in soft-matter nanostructures. Attempts to directly measure such properties, for example, by nanoindentation or a new buckling-based metrology,⁹ often are hampered by interactions with the rigid substrate^{10,11} or are unfeasible for fragile nanostructures.

Brillouin light scattering (BLS), inelastic light scattering from the acoustic phonons in a material, has proven effective for quantifying elastic properties in free-standing¹² and sup-

ported films,¹³ shallow silicon gratings,¹⁴ photonic/phononic crystals,^{15,16} and colloidal crystals.^{17,18} BLS measurements on free-standing polystyrene films showed that elastic moduli are isotropic and independent of film thickness, h , for films down to $h=29$ nm, despite a concurrent reduction of T_g in such thin films.¹² Recently, we reported the first BLS spectra for lithographically patterned photoresist lines.¹⁹ This Letter uses BLS spectroscopy, elastic wave propagation theory, and finite element analysis to identify the general forms of vibrations confined in resist nanolines. These studies lay the groundwork for an experimental methodology to characterize elastic properties and their anisotropy of two-dimensionally confined nanostructured materials.

The specimens considered in this study consist of lithographically patterned arrays of parallel lines (gratings) of a JSR²⁰ AR237 photoresist on oxidized Si substrates with an intermediate bottom antireflective coating (BARC) [Fig. 1(a)]. An unpatterned film of photoresist on the same substrate also was studied for a reference. Grating lines of length $\approx 10 \mu\text{m}$, height 320 nm, and widths w of 88 nm and 126 nm were studied. BLS spectra were measured in a back-scattering geometry at six angles θ (15° , 25° , 35° , 45° , 55° , and 67°) between the incident beam and normal to the film surface.

Figure 2 shows BLS spectra from the unpatterned film and the two gratings measured at $\theta \approx 67^\circ$. The long dimension of the polymeric lines was in the scattering plane defined by the normal and the incident beam, except for the spectrum plotted with a dotted line in Fig. 2(c), where the lines were oriented perpendicular to this plane. The polarization of the incident beam was in the scattering plane. No polarization analyzer was used for the measurements, except for spectra presented in Figs. 2(d) and 2(e) (depolarized), where the polarization perpendicular to the incident polarization was measured. The absence of visible peaks in the spectrum with the lines oriented perpendicular to the scattering plane indicates that all of the peaks arise from modes propagating along the length of the lines. Through the analysis

^{a)}Also at: IA&E, Russian Academy of Sciences, Novosibirsk, 630090, Russia.

^{b)}Author to whom correspondence should be addressed; electronic mail: alexei@uakron.edu

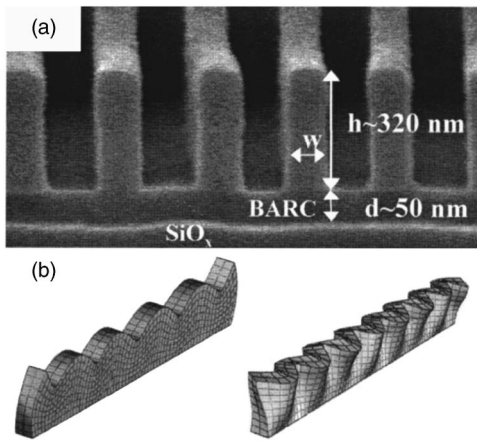


FIG. 1. (a) SEM image of photoresist gratings labeled with height (h), and width (w). The lines are supported by a layered substrate: a 50 nm bottom antireflective coating (BARC) on top of a $1 \mu\text{m}$ silicon oxide substrate. (b) Displacement patterns of the Rayleigh-type mode (left) and sub-Rayleigh mode (right).

described below, the strongest peak at a frequency ν_R of (4.29 ± 0.05) GHz from the unpatterned film and the gratings [Figs. 2(a)–2(c)] is identified with the lowest-frequency surface (Rayleigh) wave. Peaks at higher frequencies arise from higher-order surface (Sezawa) waves in the film or analogous modes in the grating lines and substrate. Surprisingly, BLS spectra of the gratings reveal a new mode below the Rayleigh mode, absent in the unpatterned film, with a frequency that depends on w [Figs. 2(b) and 2(c)]. Notice that this sub-Rayleigh (sub- R) mode is the only mode that appears in depolarized scattering spectra from the gratings [Figs. 2(d) and 2(e)], suggesting that it originates from displacements perpendicular to the side surfaces of the structures. We emphasize that such sub-Rayleigh modes are not expected for the BLS spectra of a supported film.²¹

Traditionally, the BLS modes are analyzed in terms of the dispersion of the sound velocity V calculated from the mode frequency,²²

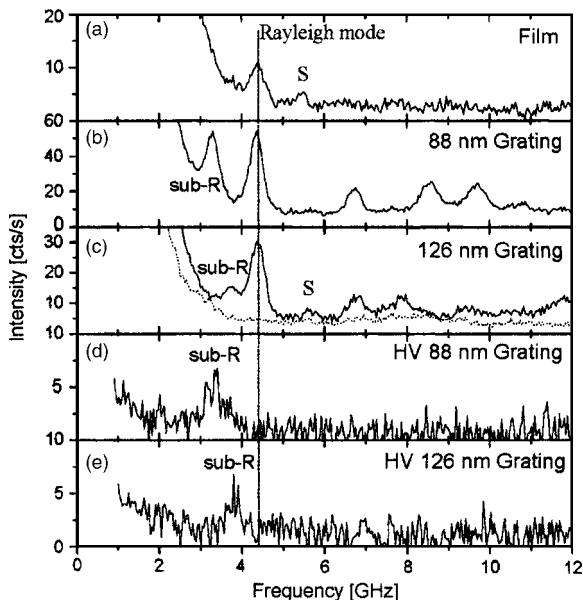


FIG. 2. Brillouin scattering spectra at $\theta=67^\circ$: (a) unpatterned film, (b) 88 nm gratings, and (c) 126 nm gratings without polarization analyzer. Spectra of scattered light polarized perpendicularly to the incident beam for (d) 88 nm gratings and (e) 126 nm gratings. Peaks from Rayleigh-type, sub-Rayleigh (sub- R) and Sezawa-type (S) modes are labeled.

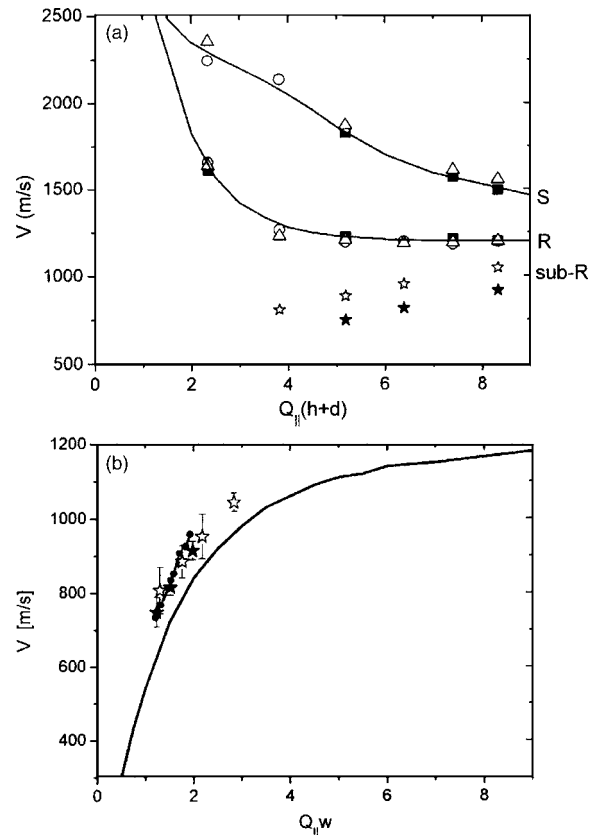


FIG. 3. Dispersion data and theoretical curves: the Rayleigh (R) and Sezawa (S) modes from a 320 nm resist thin film (squares), 88 nm grating (circles), and 126 nm grating (triangles); the sub-Rayleigh (sub- R) mode from 88 nm grating (solid stars) and 126 nm grating (hollow stars). (a) Dispersion as a function of $Q_{\parallel}(h+d)$. The solid curves show theoretical calculations of the dispersion curves for a film with $V_l=2.4$ km/s and $V_t=1.3$ km/s on a SiO_x substrate. (b) Dispersion as a function of $Q_{\parallel}w$. The solid line shows calculated dispersion for a free-standing film with the same velocities. The closed circles connected by lines are results of FE calculations for a flexural mode in the nanostructure [Fig. 1(b)]. The standard uncertainties in the experimental values of ν and V are ± 0.05 GHz and ± 0.02 km/s, respectively.

$$V \approx \frac{2\pi\nu}{Q_{\parallel}} = \frac{\nu\lambda}{2 \sin \theta}, \quad (1)$$

where $Q_{\parallel}=4\pi \sin \theta/\lambda$ is the scattering wave vector parallel to the plane of the film, and λ is the wavelength of incident light (514.5 nm). The velocities of each BLS peak are plotted in Fig. 3(a) as a function of $Q_{\parallel}(h+d)$, where $(h+d)$ is the effective film thickness, as described below.

The well-established theory of surface waves in thin films provides relationships between the velocities and wave vectors in terms of the density ρ , longitudinal V_l , and transverse V_t velocities of the film and the corresponding quantities of the substrate, ρ_s , V_{ls} , and V_{ts} .²¹ We use this theory to estimate dispersion curves for modes with wave vectors parallel to the lines. To simplify calculations, the organic BARC layer was approximated as having the same density and elastic constants as the polymeric photoresist, and the substrate was approximated as a semi-infinite silicon oxide (SiO_x). Thus, the effective film thickness of the lines is approximated as $h+d=370$ nm. The SiO_x is assumed to have the material parameters of silica (SiO_2): density $\rho_s=2.2$ g/cm³,²³ longitudinal velocity $V_{ls}=5.9$ km/s and shear velocity $V_{ts}=3.8$ km/s.²⁴ V_l of the photoresist was estimated to be (2.4 ± 0.1) km/s from the frequency spacing,

$\Delta\nu=(3.25\pm 0.10)$ GHz,¹⁹ of the longitudinal-mode BLS peaks of the unpatterned film at $\theta=8^\circ$, using the relation $V_l=2(h+d)\Delta\nu$. Since amorphous polymers typically have very similar densities, the undetermined density of the resist is taken to be that of polystyrene, 1.05 g/cm³. With V_l , ρ , V_{ls} , V_{ls} , and ρ_s fixed at these values and the asymptotic Rayleigh velocity at $V_R=(1.20\pm 0.02)$ km/s, we estimate $V_l=(1.30\pm 0.03)$ km/s. The corresponding dispersion curves are shown in Fig. 3(a), where the Rayleigh mode is labeled *R* and the lowest-order Sezawa wave is labeled *S*. These calculations agree with the BLS measurements, which indicate that the displacements of these modes in the nanolines are closely approximated by those of Rayleigh and Sezawa waves in a uniform supported film with thickness $(h+d)$.

Theory predicts²¹ that velocities of Rayleigh and Sezawa waves increase towards the substrate velocity as the phonon wavelength ($\lambda_{ph}=2\pi/Q_{||}$) becomes larger than the film thickness. In contrast to this behavior, V of the sub-Rayleigh mode decreases at low $Q_{||}$ (Fig. 3). The peculiar dispersion of the sub-Rayleigh mode is similar to the dispersion expected for the lowest-order flexural modes (Lamb waves) of a simple *free-standing* film. Rescaling the dispersion of the sub-*R* modes to the width w of the structures [Fig. 3(b)], instead of $(h+d)$ as in Fig. 3(a), results in collapse of the data for two gratings onto a single master curve, in the same manner as for Lamb waves in films of different thicknesses. Moreover, the dispersion of the sub-*R* mode is close to the dispersion expected for the Lamb mode in a free-standing film of photoresist with thickness w [Fig. 3(b)], but slightly higher, as one would expect for a structure restrained at its base by the substrate.

To explore the nature of the sub-*R* modes, finite-element (FE) analyses were performed for the resonant modes of a polymeric nanoline having a cross section of 88 nm \times 320 nm with the base fixed. The FE simulations employed a three-dimensional representation of the nanoline with a mesh of $2 \times 8 \times 64$ isoparametric brick elements and full integration on all terms. The material was assumed to be elastically isotropic. The frequencies and eigenvectors associated with each mode shape were found using the QR algorithm, which is a standard eigensolver.²⁵

A displacement pattern for one of the lowest-order flexural modes determined from these calculations is shown in Fig. 1(b). The displacements of these resonant modes are primarily perpendicular to the line directions, consistent with Figs. 2(d) and 2(e), where the sub-*R* mode is the only mode appearing in depolarized BLS spectra. Also, the corresponding phase velocities of the calculated flexural modes of the lines agree well with the experimental data [Fig. 3(b)]. This analysis reveals the microscopic nature of the new modes observed in these linear nanostructures. Moreover, it suggests that the modulus for shear displacements perpendicular to the scattering plane remains unchanged within the accuracy of our measurements ($\pm 5\%$) down to structure widths of 88 nm. These results are consistent with experiments on free-standing polystyrene films¹² and simulations of nanostructures,⁴ which do not predict significant changes in moduli at these length scales.

In conclusion, acoustic modes in polymeric nanolines have been identified from Brillouin light scattering measurements and modeling. The identification of acoustic modes with displacements along different directions provides the

basis for not only determining effective isotropic moduli, but also quantifying the anisotropy of elastic moduli arising from nanometric dimensions. While, within the accuracy of our measurements, neither changes in moduli nor anisotropies were observed in nanolines with widths down to ~ 88 nm, the potential to measure such changes now has been demonstrated.

The authors would like to thank Arpan Mahorawala for supplying the lithographically patterned nanostructures (Ref. 17), Ronald Jones for providing dimensional measurements of the nanostructures (Ref. 17), and Jack Douglas for helpful discussions and suggestions. The Akron team further acknowledges financial support from NIST, AFRL, and RFFI.

¹H. Namatsu, K. Kurihara, M. Nagase, K. Iwadate, and K. Murase, *Appl. Phys. Lett.* **66**, 2655 (1995).

²H. B. Cao, P. F. Nealey, and W.-D. Domke, *J. Vac. Sci. Technol. B* **18**, 3303 (2000).

³T. Tanaka, M. Morigami, and N. Atoda, *Jpn. J. Appl. Phys., Part 1* **32**, 6059 (1993).

⁴K. Van Workum and J. J. de Pablo, *Nano Lett.* **3**, 1405 (2003).

⁵J. L. Keddie, R. A. L. Jones, and R. A. Cory, *Europhys. Lett.* **27**, 59 (1994).

⁶J. A. Forrest, K. Dalnoki-Veress, and J. R. Dutcher, *Phys. Rev. E* **56**, 5705 (1997).

⁷D. S. Fryer, R. D. Peters, E. J. Kim, J. E. Tomaszewski, J. J. de Pablo, and P. F. Nealey, *Macromolecules* **34**, 5627 (2004).

⁸J. A. Forrest, K. Dalnoki-Veress, J. R. Stevens, and J. R. Dutcher, *Phys. Rev. Lett.* **77**, 2002 (1996).

⁹C. M. Stafford, C. Harrison, K. L. Beers, A. Karim, E. J. Amis, M. R. VanLandingham, H.-C. Kim, W. Volksen, R. D. Miller, and E. E. Simonyi, *Nat. Mater.* **3**, 545 (2004).

¹⁰C. Murray, C. Flannery, I. Streiter, S. E. Schulz, M. R. Baklanov, K. P. Mogilnikov, C. Himcinschi, M. Friedrich, D. R. T. Zahn, and T. Gessner, *Microelectron. Eng.* **60**, 133 (2002).

¹¹M. R. VanLandingham, J. S. Villarrubia, W. F. Guthrie, and G. F. Meyers, *Macromol. Symp.* **167**, 15 (2001).

¹²J. A. Forrest, K. Dalnoki-Veress, and J. R. Dutcher, *Phys. Rev. E* **58**, 6109 (1998).

¹³L. Sun, J. R. Dutcher, L. Giovanni, F. Nizzoli, J. R. Stevens, and J. L. Ord, *J. Appl. Phys.* **75**, 7482 (1994).

¹⁴J. R. Dutcher, S. Lee, B. Hillebrands, G. J. McLaughlin, B. G. Nickel, and G. I. Stegeman, *Phys. Rev. Lett.* **68**, 2464 (1992).

¹⁵A. M. Urbas, E. L. Thomas, H. Kriegs, G. Fytas, R. S. Penciu, and L. N. Economou, *Phys. Rev. Lett.* **90**, 108302 (2003).

¹⁶T. Gorishnyy, C. K. Ullal, M. Maldovan, G. Fytas, and E. L. Thomas, *Phys. Rev. Lett.* **94**, 115501 (2005).

¹⁷M. H. Kuok, H. S. Lim, S. C. Ng, N. N. Liu, and Z. K. Wang, *Phys. Rev. Lett.* **90**, 255502 (2003).

¹⁸R. S. Penciu, H. Kriegs, G. Petekidis, G. Fytas, and E. N. Economou, *J. Chem. Phys.* **118**, 5224 (2003).

¹⁹R. Hartschuh, Y. Ding, J. H. Roh, A. Kisliuk, A. P. Sokolov, C. L. Soles, R. L. Jones, T. J. Hu, W. L. Wu, and A. P. Mahorawala, *J. Polym. Sci., Part B: Polym. Phys.* **42**, 1106 (2004).

²⁰Certain commercial equipment and materials are identified in this paper in order to specify adequately the experimental procedure. In no case does such identification imply recommendation by the National Institute of Standards and Technology nor does it imply the material or equipment identified is necessarily the best available for this purpose.

²¹G. W. Farnell and E. L. Adler, in *Physical Acoustics, Principles and Methods*, edited by W. P. Mason and R. N. Thurston (Academic, New York, 1972), Vol. 9, pp. 35–87.

²²F. Nizzoli and J. R. Sandercock, in *Dynamical Properties of Solids*, edited by G. K. Horton and A. A. Maradudin (Elsevier, Amsterdam, 1990), Vol. 6, pp. 281–335.

²³A. J. Garcia and J. Fernandez, *Phys. Rev. B* **55**, 5546 (1997).

²⁴I. L. Fabelinsky, *Molecular Scattering of Light* (Plenum, New York, 1968).

²⁵L. Meirovitch, *Computational Methods in Structural Dynamics* (Sijthoff and Noordhoff, Rockville, MD, 1980).